Factors Contributing to Binding-Site Imperfections in Imprinted Polymers

Irena Yungerman and Simcha Srebnik*

Department of Chemical Engineering, Technion—Israel Institute of Technology, Haifa, Israel 32000

Received March 17, 2005. Revised Manuscript Received October 27, 2005

The quality of molecularly imprinted polymers depends on the ability to form molecule-specific recognition sites within the host gel. We investigate the imprinting quality of cross-linked polymer networks using molecular dynamics simulations through a topological analysis of the imprinted network configuration before and after removal of the templates. We define a measure for the quality of the imprinted polymer on the basis of the shape and size of the imprinting-induced binding sites. Low qualities of the imprinted gels are attributed to aggregation of the templates in the prepolymerization solution, aggregation of the imprinting-induced sites with small pores inherent to the gel, and deformation of the binding sites due to relaxation of the gel after removal of the templates. The formation of distinct individual cavities that retain the size and shape of the template is enhanced by high degrees of cross-linking and low template concentrations, in agreement with experimental observations.

1. Introduction

Molecular imprinting is a simple technique that can, in principle, achieve molecule-specific recognition on the basis of morphology and/or stereochemistry. The most versatile technique, developed by Mosbach,[1] involves noncovalent binding and rebinding of the molecular-recognition agents to the imprinted cavities of the molecularly imprinted polymer (MIP), as illustrated in Figure 1.

Molecular imprinting has gained substantial attention as a means for achieving functional materials for applications, including molecule-specific separations,[2,3] catalysis,[4] and chiral technologies.[5] In particular, the existence of a large number of functional groups in a small volume of material makes MIPs important for use in biological and pharmaceutical applications,[6,7] such as the use of entrapped proteins as biosensors or biocatalysts, diffusion-controlled release of proteins, or the design of systems that can be targeted toward undesirable compounds.

The quality (of the polymerization reaction) and performance (rebinding ability) of the imprinted gel rely on careful tailoring of the physical and chemical nature of the monomers and the interactions between them, the polymerization reaction and its affect on the porous structure, and the rebinding ability of the imprinted cavities. A notable drawback with recognition-based applications of MIPs is the low yields of high-affinity sites. Regrettably, only a relatively small number of research groups focus on characterizing and understanding the mechanisms underlying formation of MIPs,[7−27] with practically all of them concentrating mainly on template-functional monomer ratios[11−17] and the nature of the binding site interactions,[17−25] with only minor treatment of the macro- and microstructure of the porous network.[7−11] It has become apparent that the quantity and quality of MIP recognition sites is a direct function of the nature and extent of the monomer−template interactions present in the prepolymerization mixture. Whereas binding-assay studies are used to characterize the functionality of the formed imprinted cavities, structural studies are necessary

* To whom correspondence should be addressed. E-mail: simchas@techunix.technion.ac.il.

(1) Arshady, R.; Mosbach, K. *Makromol. Chem.* **1981**, *182*, 687.
(2) Haupt, K.; Mosbach, K. *Trends Biotechnol.* **1998**, *16*, 468.
(3) Piletsky, S. A.; Panasyuk, T. L.; Piletskaya, E. V.; Nicholls, I. A.; Ulbricht, M. *J. Membr. Sci.* **1999**, *157*, 263.
(4) Freemantle, M. *Chem. Eng. News* **2000**, *78*, 31.
(5) Kempe, M.; Mosbach, K. *J. Chromatogr., A* **1995**, *694*, 3.
(6) Ratner, B. D.; Shi, H. Q. *Curr. Opin. Solid State Mater. Sci.* **1999**, *4*, 395.
(7) Byrne, M. E.; Park, K.; Peppas, N. A. *Adv. Drug Delivery Rev.* **2002**, *54*, 149.
(8) Shea, K. J.; Dougherty, T. K. *J. Am. Chem. Soc.* **1986**, *108*, 1091.
(9) Shea, K. J.; Sasaki, D. Y. *J. Am. Chem. Soc.* **1989**, *111*, 3442.
(10) Turner, N. W.; Piletska, E. V.; Karim, K.; Whitcombe, M.; Malecha, M.; Magan, N.; Baggiani, C.; Piletsky, S. A. *Biosens. Bioelectron.* **2004**, *20*, 1060.
(11) Baggiani, C.; Anfossi, L.; Giovannoli, C.; Tozzi, C. *Talanta* **2004**, *62*, 1029.
(12) Andersson, H. S.; Nicholls, I. A. *Bioorg. Chem.* **1997**, *25*, 203.
(13) Andersson, H. S.; Karlsson, J. G.; Piletsky, S. A.; Koch-Schmidt, A. C.; Mosbach, K.; Nicholls, I. A. *J. Chromatogr., A* **1999**, *848*, 39.
(14) Chen, W. Y.; Chen, C. S.; Lin, F. Y. *J. Chromatogr., A* **2001**, *923*, 1.
(15) Ansell, R. J.; Kuah, K. L. *Analyst* **2005**, *130*, 179.
(16) Fish, W. P.; Ferreira, J.; Sheardy, R. D.; Snow, N. H.; O'Brien, T. P. *J. Liq. Chromatogr. Rel. Tech.* **2005**, *28*, 1.
(17) Berglund, J.; Nicholls, I. A.; Lindbladh, C.; Mosbach, K. *Bioorg. Med. Chem. Lett.* **1996**, *6*, 2237.
(18) Sellergren, B.; Lepisto, M.; Mosbach, K. *J. Am. Chem. Soc.* **1988**, *110*, 5853.
(19) Andersson, L. I.; Muller, R.; Vlatakis, G.; Mosbach, K. *Proc. Natl. Acad. Sci. U.S.A.* **1995**, *92*, 4788.
(20) Andersson, H. S.; KochSchmidt, A. C.; Ohlson, S.; Mosbach, K. *J. Mol. Recognit.* **1996**, *9*, 675.
(21) Wulff, G. *Mol. Cryst. Liq. Cryst. Sci. Technol., Sect. A* **1996**, *276*, 1.
(22) Matsui, J.; Kubo, H.; Takeuchi, T. *Anal. Sci.* **1998**, *14*, 699.
(23) Piletsky, S. A.; Andersson, H. S.; Nicholls, I. A. *J. Mol. Recognit.* **1998**, *11*, 94.
(24) Zhang, T. L.; Liu, F.; Chen, W.; Wang, J.; Li, K. *Anal. Chim. Acta* **2001**, *450*, 53.
(25) Huang, X. D.; Kong, L.; Li, X.; Zheng, C. J.; Zou, H. F. *J. Mol. Recognit.* **2003**, *16*, 406.
(26) Oral, E.; Peppas, N. A. *Polymer* **2004**, *45*, 6163.
(27) Byrne, M. E.; Oral, E.; Hilt, J. Z.; Peppas, N. A. *Polym. Adv. Technol.* **2002**, *13*, 798.

10.1021/cm050598f CCC: $33.50
Published on Web 01/07/2006

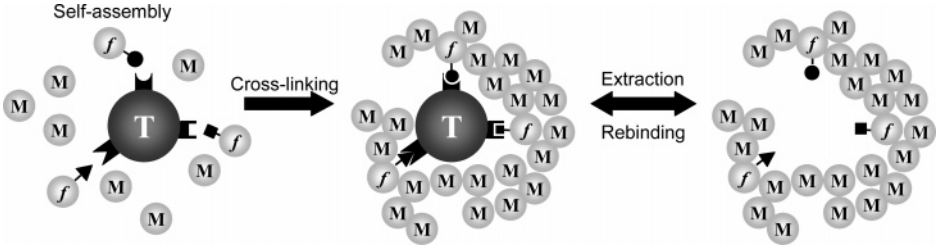

Figure 1. Schematic of the three main steps of molecular imprinting: (1) Functional monomers (f) are allowed to self-assemble around the template (T). (2) Polymerization and cross-linking of the monomers (M) around the template-functional monomer complex proceeds until a rigid gel is formed. (3) Extraction (rebinding) of the template from (to) the imprinted binding sites.

in order to characterize the influence of size and shape on imprinting performance. A reason for the lack of structural studies is the problematic analysis of the porous structure of the MIP, which is not amenable to X-ray crystallography or microscopic techniques because of its amorphous and heterogeneous nature. Thus, little is known about the molecular-level events that determine the imprinting quality and performance.

Several general guidelines for fabricating stable imprinted gels emerge from these studies: It is generally believed that highly cross-linked (70−90%) rigid polymers are needed to maximize binding-site integrity, yet some degree of flexibility is needed to allow for rebinding of the imprinting agent. In fact, it has become apparent that lower degrees of cross-linking that result in more flexible materials can also display significant affinity toward the print molecules.[28−30] In addition, it has been observed that the difficulty in fabricating imprinted materials increases with increasing concentration and size of the imprinting agent.

Theoretical models of MIPs have mainly focused on qualitative thermodynamic and kinetic arguments[18,31] to shed light on observed recognition behavior or have suggested new imprinting methods.[32,33] Our group has been involved in the structural characterization of MIPs using statistical thermodynamic models.[34,35] We also studied the effects of the size of the imprinting agent (template) and solvent−template−monomer interactions on the imprinting quality using a reaction kinetics lattice model.[36]

Computational studies are even less prevalent in the literature. Recently, an ab initio simulation was used to study the binding energy between the monomer and template.[37] Molecular dynamics simulations were used to screen between a large number of functional monomers to select those that interact most with the template, which were chosen for the preparation of a MIP.[38] In this work, we study the structure of polymer gels made up of tetrafunctional monomers formed in the presence of rigid dumbbell-like nonfunctional templates using molecular dynamics simulations. We simulate the gelation of monomers in the presence of the templates followed by relaxation of the gel once the templates have been removed. We compare the distribution of the templates with the formed binding sites before and after network relaxation and obtain a measure for the quality of imprinting. To concentrate on structural changes in the structure of imprinted cavities due to removal of the templates, we neglect specific molecular interactions between the templates, cross-linkers, and monomers. Such issues will be taken up in later studies.

The remainder of the paper is organized as follows. In section 2, we describe our simulation method used to generate the imprinted gel. We detail the algorithm used to characterize the structure of the gel at various stages of the simulation. In section 3, we present and discuss our results. We introduce a simple measure for the quality of the imprinted gel and analyze the different mechanisms that lead to poor imprinting qualities. We offer concluding remarks in section 4.

2. Methodology

2.1. Molecular Dynamics Simulation. It has become apparent that two key features that reduce the quality of MIPs are the insufficient complexation of print molecules with the functional monomers in the prepolymerization step and the relaxation of the polymer network once the print molecules have been removed. Whereas the former leads to low functional specificity, local relaxation leads to lower shape complementarity between the binding sites and print molecules. In this work, we focus on the latter, in hopes of elucidating the factors leading to poor shape recognition. Furthermore, we do not consider other factors, such as solvent, local temperature gradients, and phase separation induced by uneven distribution of cross-links. These contributions are expected to reinforce the results observed with the current simplified simulations.

We adapt the Gen_Pol[39] package, a coarse-grained molecular dynamics simulation of polymers, to simulate polymerization and cross-linking of the functional monomers around nonfunctional dumbbell-like dimeric print molecules. Gen_Pol allows for the efficient generation of concentrated polymer solutions using a Monte Carlo procedure based on the canonical ensemble. The solution is then equilibrated by a standard microcanonical molecular dynamics

(28) Yilmaz, E.; Mosbach, K.; Haupt, K. *Anal. Commun.* **1999**, *36*, 167.
(29) Yu, C.; Mosbach, K. *J. Chromatogr., A* **2000**, *888*, 63.
(30) Yilmaz, E.; Mosbach, K.; Haupt, K. *Anal. Commun.* **1999**, *36*, 167.
(31) Nicholls, I. A.; Adbo, K.; Andersson, H. S.; Andersson, P. O.; Ankarloo, J.; Hedin-Dahlstrom, J.; Jokela, P.; Karlsson, J. G.; Olofsson, L.; Rosengren, J.; Shoravi, S.; Svenson, J.; Wikman, S. *Anal. Chim. Acta* **2001**, *435*, 9.
(32) Pande, V. S.; Grosberg, A. Y.; Tanaka, T. *Proc. Natl. Acad. Sci. U.S.A.* **1994**, *91*, 12976.
(33) Enoki, T.; Tanaka, K.; Watanabe, T.; Oya, T.; Sakiyama, T.; Takeoka, Y.; Ito, K.; Wang, G. Q.; Annaka, M.; Hara, K.; Du, R.; Chuang, J.; Wasserman, K.; Grosberg, A. Y.; Masamune, S.; Tanaka, T. *Phys. Rev. Lett.* **2000**, *85*, 5000.
(34) Srebnik, S.; Lev, O. *J. Chem. Phys.* **2002**, *116*, 10967.
(35) Srebnik, S.; Lev, O.; Avnir, D. *Chem. Mater.* **2001**, *13*, 811.
(36) Srebnik, S. *Chem. Mater.* **2004**, *16*, 883.
(37) Wu, L. Q.; Sun, B. W.; Li, Y. Z.; Chang, W. B. *Analyst* **2003**, *128*, 944.
(38) Subrahmanyam, S.; Piletsky, S. A.; Piletska, E. V.; Chen, B. N.; Karim, K.; Turner, A. P. F. *Biosens. Bioelectron.* **2001**, *16*, 631.
(39) Kroger, M. *Comput. Phys. Commun.* **1999**, *118*, 278.

routine that integrates Newton's equations of motion using the standard Verlet algorithm. We modified the package to simulate heterogeneous solutions and cross-linking.

In our current study, we consider the simple problem of rigid dimers as the imprinting agent, or template, for elucidating basic physics governing poor imprinting quality due to network relaxation. The monomers making up both the template and polymer are modeled as Lennard-Jones (LJ) spheres with radius σ that interact through short-range forces of strength, ϵ, truncated at a short distance to impose mainly repulsive interactions.

$$U_{\mathrm{LJ}}(r) = 4\epsilon\left[\left(\frac{\sigma}{r}\right)^6 - \left(\frac{\sigma}{r}\right)^{12}\right] - U_{\mathrm{LJ}}(r_{\mathrm{cut}}) \text{ if } r \le r_{\mathrm{cut}},\ U_{\mathrm{LJ}}(r) = 0 \text{ if } r > r_{\mathrm{cut}} \quad (1)$$

The bonds between neighboring monomers obey the Fene potential and harmonic cosine bending potential, respectively

$$U_{\mathrm{FENE}}(r) = -\frac{1}{2}kR_0^2 \ln\left(1 - \left(\frac{r}{R_0}\right)^2\right) \text{ if } r < R_0,\ U_{\mathrm{FENE}}(r) = \infty \text{ if } r \ge R_0 \quad (2)$$

$$U_{\mathrm{bend}}(r) = \frac{1}{2}\kappa(\cos\theta - \cos\theta_0)^2 \quad (3)$$

where k is the spring constant, R_0 is the equilibrium bond length, κ is the bending constant, and θ_0 is the equilibrium angle. All parameters are provided in LJ units, such that distances are normalized by the LJ parameter corresponding to monomer size, σ (e.g., CH_2 or SiO_2), and energies are normalized by the LJ parameter ϵ. Molecular masses are normalized by the monomer's atomic mass.

Initially, the monomers and print molecules are randomly placed in the simulation box. The solution is equilibrated, and cross-linking is performed to the desired degree of cross-linking, *f*. Monomers of quadruple functionality are considered. The cross-linking sites are randomly chosen between monomers that are in proximity. This process corresponds, for example, to instantaneous cross-linking by irradiation or by other means, whereby a fraction of all monomers at a distance on the order of σ (i.e., contacting monomers) cross-link irreversibly. Though in practice the chain-building monomers are difunctional, cross-linking monomers are in general chosen to have reactivites similar to that of the chain-building monomers in order to produce a homogeneous network with spatially even cross-linking density. The angles between the cross-linked monomers obey eqs 2 and 3. The system is equilibrated before and after the templates are removed.

2.2. Characterization of the Imprinted Gel. Several parameters determine the efficiency, or ability of the imprinting process to retain characteristics complementary to the templates, including a rigid polymer gel (obtained through a high degree of cross-linking), aggregation of the templates, and relaxation of the polymer after removal of the templates. To estimate the efficiency of the imprinting process, we investigate the overall pore-size distribution and the imprinting-induced binding-site distribution, as well as the spatial arrangement of the templates.

We study the effects of the equilibrium process as a function of various parameters by analyzing equilibrium configurations of the gel before and after removal of the print molecules. The following algorithm was developed to identify and characterize the pore structure of the resulting gel configurations.[2] First, the molecular configuration, obtained from the simulation as a set of coordinates of the centers of molecules, is transformed into a binary image by partitioning the simulation box into a grid of a specified mesh size. Cells that overlap with particles are labeled as 1, whereas cells that do not overlap with particles are labeled as 0. In this manner, the configurational space is stored in a one-dimensional binary array of length *M*, where *M* is the number of grid cells. Once the preliminary binary occupancy image has been created, the porous structure is analyzed in terms of pore connectivity and bottlenecks, which are used to determine pore size. The algorithm consists of first identifying individual pores, defined by bottlenecks according to a specified criterion. The algorithm automatically stores the number of cells belonging to each pore and their spatial location. Subsequently, the pore-size distribution and any other spatial characteristics of the porous structure are easily obtained.

3. Results and Discussion

In this work, we consider imprinting according only to shape and size. Our goal is to examine the effects of template size and the degree of cross-linking on imprinting quality, determined by the deformation of the imprinted polymer network and degree of aggregation of the templates. The following discussion analyzes the results of simulation runs of polymerization and cross-linking of 4500−4950 tetrafunctional monomers, in the presence of 25−250 template molecules made of 2 monomers each. The degree of cross-linking is varied between 50 and 90%. The average density is 1.0 σ^{-3} in all simulations. The simulated imprinting process begins with the equilibration of the functional monomers in the presence of the templates followed by cross-linking and equilibration. Subsequently, the templates are removed, and the system is once again equilibrated.

In our analysis of the porous structure, we divide the cavities in the material into three types: (1) template-induced binding sites that retain the shape and size of the imprinting agent, (2) "background" pores present in the gel because of inherent local density fluctuations in the polymer gel, and (3) cavities induced by rearrangement of the imprinted binding sites after equilibration of the gel once the templates have been removed. To differentiate between these types of cavities, we follow the final molecular configuration as well as the equilibrated configuration before the templates are removed. Our analysis is carried out by projecting the off-lattice configuration onto a fine lattice (as described in Methodology). Comparison between these images enables the differentiation between the two types of template-induced binding sites (types 1 and 3) as well as the reorganization of background pores, thereby obtaining an accurate pore-size distribution and a measure of the imprinting quality.

The pore-size distributions for various template concentrations and degrees of cross-linking are shown in Figure 2. For comparison, distributions of the degree of aggregation of the imprinting molecules before their removal are shown in Figure 3. All distributions presented are averages over 10 simulation runs. From the plots in Figure 2, it is apparent that in the case of 70 and 90% cross-links at all concentrations (15% concentration of templates being a possible exception), the maximum pore-size distribution is, as expected, equal to the size of a single template ($2\sigma^3$), whereas in the case of 50% cross-links, a significant concentration of small pores that are an order of magnitude smaller than the templates exists, particularly at concentrations less than 5%. In all three cases, high template capacities result in extremely poor imprinting, indicated by low concentrations

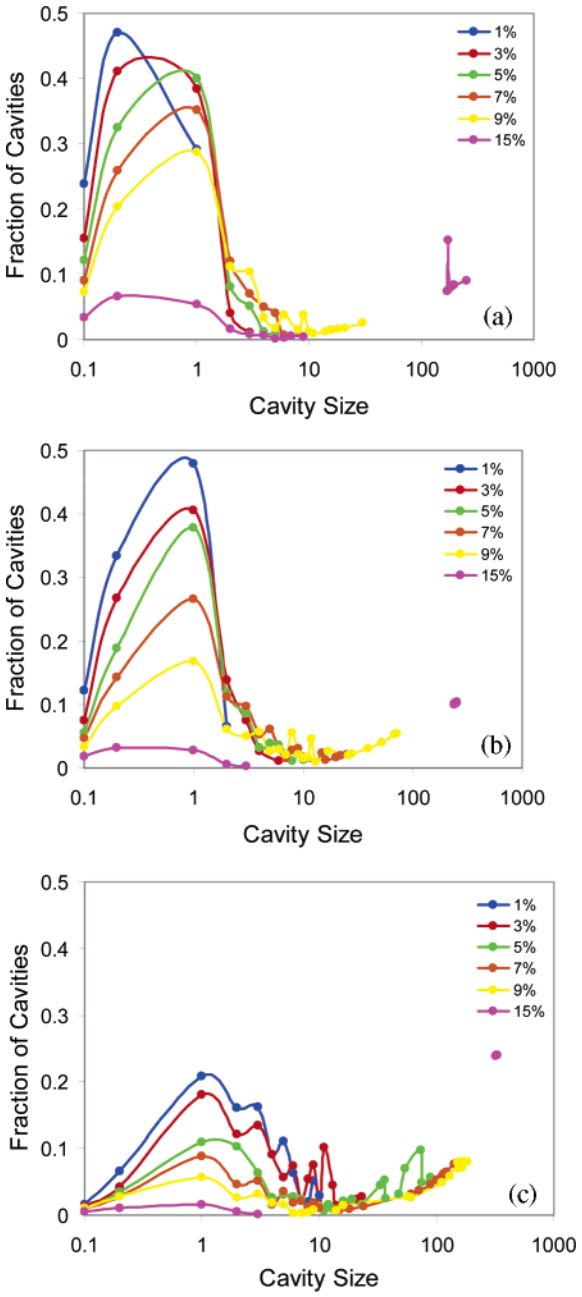

Figure 2. Size distributions of cavities obtained from simulated configurations at different percent compositions of imprinting molecules each having a volume of $2\sigma^3$. The cavity size is normalized by the size of an imprinting molecule: (a) 50% polymer cross-linking, (b) 70% polymer cross-linking, and (c) 90% polymer cross-linking.

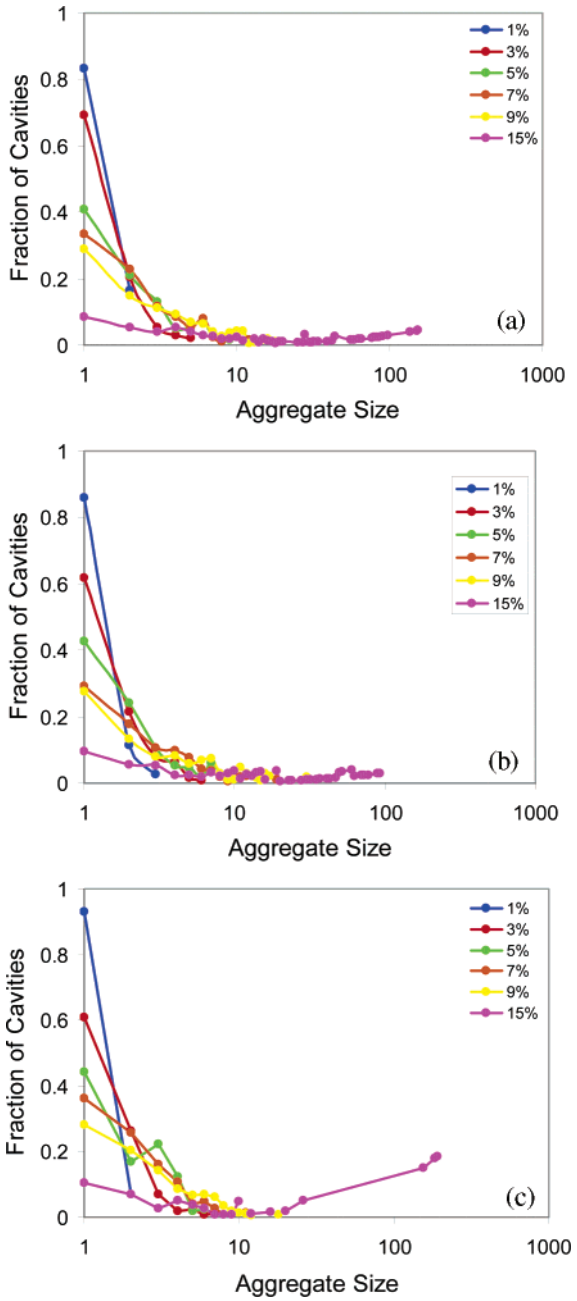

Figure 3. Degree of aggregation of templates at different percent compositions, each having a volume of $2\sigma^3$ (the size of a template aggregate in relation to the size of a template); (a) 50% polymer cross-linking, (b) 70% polymer cross-linking, and (c) 90% polymer cross-linking.

of template-sized cavities combined with a high tendency to form very large cavities. Another clear trend that is common to Figure 2a−c is the decreased quality of the MIPs (measured here by pore volume only, without shape considerations) with increased template capacities. This trend has also been observed experimentally.[30]

In case of a very high degree of cross-linking (90%) we observe the formation of increasingly larger cavities, presumably formed by large template aggregates as the concentration of imprinting molecules is increased. Indeed, Figure 2 reveals that a high degree of cross-linking appears to increase aggregation, particularly at high template fractions. This, however, is an artifact of the analysis according to pore size without considering the shape of the pores. The picture that emerges is the following: During cross-linking, a large fraction of monomers are forced to link in a frozen conformation, leading to constrained bonds, especially in the vicinity of the templates. Thus, local fluctuations in the monomer and template densities are enhanced because high monomer density areas are cross-linked, whereas monomers in the vicinity of templates are less likely to cross-link. Equilibration of the system after template removal leads to relaxation of the network, where cavities formed by template aggregates may reshape to smaller ones for low degrees of cross-linking, resulting in smaller overall pore sizes. Highly cross-linked gels, however, retain the shape of the template-induced cavities, including large ones formed by template aggregates.

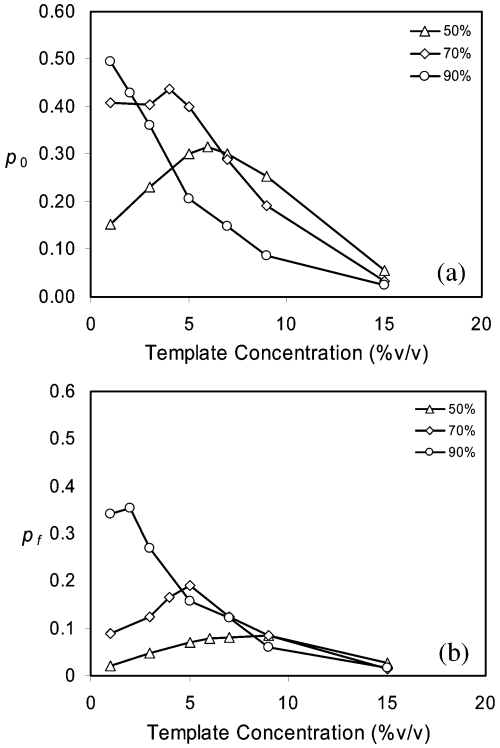

Figure 4. Imprinting performance calculated according to (a) cavity size only and (b) cavity shape and size as a function of percent composition of templates. Curves correspond to different degrees of cross-linking.

An interesting trend is observed by comparing Figures 2 and 3 for lower degrees of cross-linking (50−70%). The fraction of pores that correspond to a template molecule equals the fraction of templates that are not aggregated for intermediate template concentrations (∼5−9%). However, as we argue below, this again is a result of the breaking of large pores into smaller ones during the final equilibration of the template-free network.

Although the distributions in Figure 3 in general are quantitatively similar for the different degrees of cross-linking, those in Figure 2 are not. Apparently, postequilibration of the system after removal of the templates significantly alters the pore structure. The pore-size distributions in the absence of the templates appear to lead to a dramatically lower maximal imprinting quality as the degree of cross-linking is increased, particularly for high template concentrations. A physical explanation for this trend can be obtained when the shapes of the imprinting-induced cavities are considered in addition to their volumes.

First, we define a measure for the quality of the imprinting process, q_0, through the ratio of the real volume of cavities of approximate targeted size (in our analysis below, a range of $0.5(2\sigma^3)$ to $1.5(2\sigma^3)$ was admitted), v_q, to the real total volume of imprinting molecules, v_{im}, present in the preparation solution

$$\%q_0 = \frac{v_q}{v_{im}} \times 100 \qquad (4)$$

However, it is not sufficient to consider only pore size, because, as we shall show, network relaxation may lead to cavities with the targeted volume (that are not necessarily imprinting-induced) but not the shape of the template.

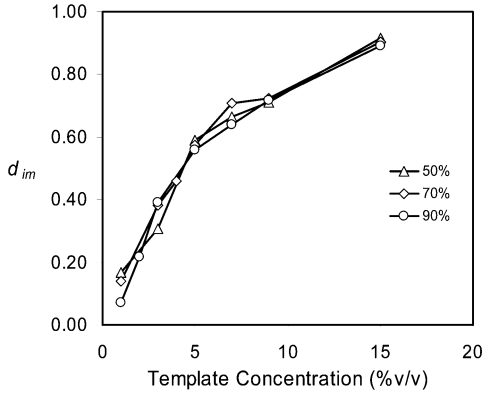

Figure 5. Aggregation parameter d_{im} as a function of percent template concentration for different degrees of cross-linking.

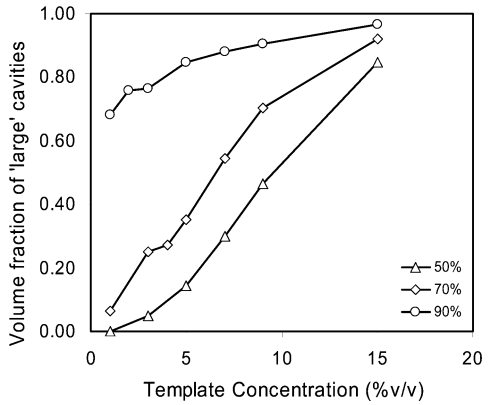

Figure 6. Concentration of cavities in the imprinted solid that are greater than the size of a single template as a function of template concentration, for different degrees of cross-linking.

Therefore, we calculate an additional quantity, q_f, that provides a measure of imprinting quality on the basis of the size and shape of the imprinting-induced pores

$$\%q_f = \frac{v_{qf}}{v_{im}} \times 100 \qquad (5)$$

where v_{qf} is the volume of the cavities of targeted size and shape, i.e., potential binding sites. Qualities of the imprinting process, calculated according to eqs 4 and 5 as a function of the template concentration ratio, are plotted in panels a and b of Figure 4, respectively.

As can be observed from Figure 4a, there is an optimum value of the percent composition of the imprinting molecules at which quality is maximal, which decreases with increasing degrees of cross-linking. We notice similar trends for imprinting quality when the cavity size and shape are accounted for. However, comparison between the two plots (4a and 4b) reveals that the overall imprinting quality is decreased at all degrees of cross-linking and for the entire range of template concentrations tested when both the size and shape of the imprinting-induced cavities are taken into account but less so with an increasing degree of cross-linking. Significantly, q_f approaches q_0 at 90% cross-links, as expected, because highly cross-linked gels are rigid and thus retain their structure.

Thus, from our discussion of Figures 2−4, we can conclude that pore-size distribution is an insufficient measure for imprinting quality, and may in fact be misleading. That

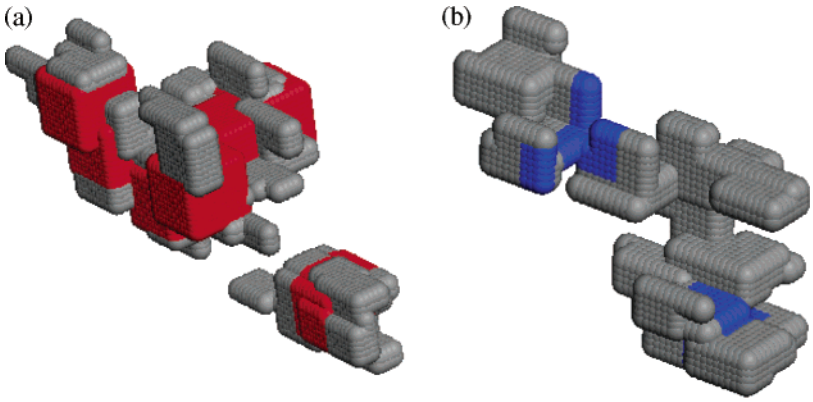

Figure 7. Illustration of pore formation and deformation during different stages of the imprinting process at a 50% degree of cross-linking. (a) Two different cavities form around template clusters and a single template after cross-linking; (b) significant deformation of the template-induced cavity is observed after template removal, mainly for the aggregate, resulting in a large pore that will show poor recognition. Gray indicates pores due to density fluctuations of the gel; red indicates templates prior to their removal, and blue indicates template-induced cavities after equilibration.

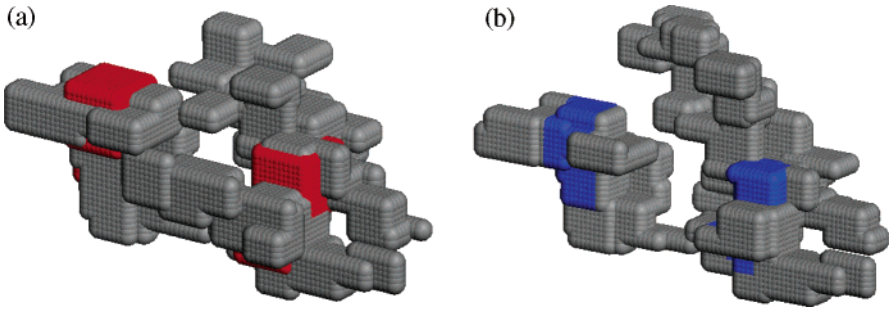

Figure 8. Illustration of cavity formation and deformation during different stages of the imprinting process at a 90% degree of cross-linking. (a) Two templates connected through narrow channels after cross-linking of the polymer; (b) removal of the templates does not lead to significant deformation of the cavities. Gray indicates pores due to density fluctuations of the gel; red indicates templates prior to their removal, and blue indicates template-induced cavities after equilibration.

is, Figure 2 suggests that a much smaller fraction of pores retain the desired volume at 90% cross-linking than at 50 and 70%. However, when both pore size and shape are considered, we find that 90% cross-linked networks show the best imprinting quality.

To clarify the process that leads to cavity formation and deformation, we examine the degree of aggregation of the templates. We define an aggregation parameter, d_{im}, which measures the degree of aggregation such that

$$d_{im} = \frac{\sum_{ag} n_{ag} v_{ag}}{v_{im}} \tag{6}$$

where n_{ag} is the number of aggregated groups of size v_{ag} ($>2\sigma^3$) and v_{im} is the total volume of the templates. The aggregation parameter d_{im}, which represents the total fractional volume of template aggregates, is plotted as a function of template concentration ratio in Figure 5. For comparison, we include a graph of the concentrations of cavities whose size is greater than that of a single template in Figure 6. It is noteworthy that the templates show the same degree of aggregation at all degrees of cross-linking considered. Clearly, template aggregation occurs prior to the polymerization process and does not continue once the gel has formed. It may be further concluded that even at 50% cross-links, spatial rearrangement of the templates within the gel is limited to local movements. The trend of increasing template complexation with increasing capacities might explain the observed increased nonspecific binding of templates.[13]

The observation in Figure 6 that the fraction of large cavities increases with template concentration but is larger for higher degrees of cross-linking allows us to conclude that relaxation of the less-rigid networks leads to the breaking of large cavities (which are induced by template aggregates) into smaller ones, some of which correspond in size to a single template molecule, giving the appearance of a higher imprinting quality at a lower degree of cross-linking if only cavity size is considered. This is illustrated in Figures 7 and 8, in which the formation and deformation of specific cavities were followed through the various equilibration steps in our simulation.

From our analysis, it is apparent that the shift of p_f toward higher template concentrations with decreasing degrees of cross-linking (albeit with decreasing overall quality), as seen in Figure 4, is due to two opposing processes: (1) aggregation of templates, which increases with template concentration, and (2) relaxation of the network, which decreases with an increasing degree of cross-linking. That is, by relaxing the bigger cavities formed from template aggregates, the gel becomes less strained; however, this relaxation is inhibited by higher degrees of cross-linking.

4. Conclusions

Successful molecular imprinting requires the presence of a sufficient number of binding sites of a particular targeted shape and size. In practice, a 5−10% imprinting concentration ratio is used[41] with an efficiency as low as 15% (i.e., only 15% of the binding sites show retake of the template).

We find that aggregation of the templates in the prepolymerization solution contributes significantly to poor imprinting qualities, leading to imprinting qualities of 10−15%, which is nearly independent of the degree of cross-linking at concentration ratios of ≥10%. Lower template capacities suffer significantly from local rearrangement of the cavities at lower degrees of cross-linking, resulting in significant deformation of the binding sites and lower imprinting qualities. While some degree of the shape complementarity exhibited by the imprinted polymer arises from cross-linking, it is apparent that other factors must be included in order to have precise control over the structure of the imprinted cavities. Our analysis suggests that effective imprinting demands lower degrees of aggregation. Although it has been suggested that the real molecular-recognition mechanism involves clusters of template molecules being packed into the binding site,[42] this may not suffice when molecule-specific recognition is required. These results are significant for applications such as binding assays, imprinted hydrogels,[27] or bulk separations, where it is becoming apparent that greater flexibility can improve the imprinting concentration ratio.

In future work, we will examine the role of functional sites on imprinting quality. We expect functionality to increase imprinting quality by impeding aggregation but also to decrease quality, as not all cavities will be fully functional.[19,30,36]

Acknowledgment. This research was supported by the Israel Science Foundation, the Steven and Nancy Grand Water Research Institute, and the Center for Absorption in Science, Ministry of Immigrant Absorption, State of Israel.

CM050598F

(40) We note that a similar algorithm has been published recently: Ye, G.; van Breugel, K.; Fraaij, A. L. A. *Cem. Concr. Res.* **2003**, *33*, 215. However, it is more complex and more computationally expensive than our suggested algorithm.

(41) Wulff, G.; Knorr, K. *Bioseparation* **2002**, *10*, 257.

(42) Sellergren, B.; Shea, K. J. *J. Chromatogr.* **1993**, *635*, 31.